

Article

Design of a High-Voltage Insulation Resistance Detection System for Commercial Vehicles

Feng Guo ^{1,2,3}, Danping She ^{2,3}, Xinfeng Zhang ^{1,*} and Yue Han ¹

¹ School of Information and Electrical Engineering, Hangzhou City University, Hangzhou 310015, China; guof22@sany.com.cn (F.G.); 22302003@stu.hzcu.edu.cn (Y.H.)

² Hunan New Energy Heavy Truck Power Systems Engineering Technology Research Center, Changsha 410000, China; shedp@sany.com.cn

³ Hunan Xingbida Wanglian Technology Co., Ltd., Changsha 410000, China

* Correspondence: zxf@hzcu.edu.cn

Abstract: Based on the safety monitoring requirements of power batteries for new energy commercial vehicles, this study proposes a battery insulation detection method utilizing the bridge method in combination with existing insulation detection techniques. Through optimization and improvement of this methodology, an insulation detection system for new energy commercial vehicle power batteries was developed, along with a dynamic online calculation method for insulation resistance. Comprehensive experimental testing under multiple operational conditions demonstrates that the proposed system achieves a measurement accuracy with errors below 5% for insulation resistance. Furthermore, the system exhibits significant advantages in dynamic real-time monitoring capabilities and operational reliability.

Keywords: electric commercial vehicle; power battery; insulation test; unbalanced bridge test

1. Introduction



Academic Editor: Marco Giorgetti

Received: 24 February 2025

Revised: 25 March 2025

Accepted: 29 March 2025

Published: 7 April 2025

Citation: Guo, F.; She, D.; Zhang, X.; Han, Y. Design of a High-Voltage Insulation Resistance Detection System for Commercial Vehicles. *Batteries* **2025**, *11*, 143. <https://doi.org/10.3390/batteries11040143>

Copyright: © 2025 by the authors. Licensee MDPI, Basel, Switzerland. This article is an open access article distributed under the terms and conditions of the Creative Commons Attribution (CC BY) license (<https://creativecommons.org/licenses/by/4.0/>).

With the requirement of the dual-carbon strategy, the development of electric vehicles is necessary for sustainable transportation and upgrading the global automotive industry. China's traditional automotive enterprises have overtaken passenger cars in terms of electrified technology. However, commercial vehicles are still following suit to start the electrification era. Most electric vehicles (EVs) utilize high-voltage lithium-ion batteries as their power source [1–3]. Given that high-voltage lithium-ion batteries are part of a high-voltage direct current (HVDC) system, the high-voltage insulation performance of the vehicle is of great significance to the safe operation of electric vehicles [4–6]. But electric commercial vehicles also use lithium batteries as their energy source, and the voltage platform is much higher (more than 800 V). This high-voltage level can be very dangerous to personal safety. The operating conditions and environments of electric vehicles, including high-temperature, high-humidity, and high-salinity fog environments, are highly complex [7–11]. Under these conditions, high-voltage electrical components may exhibit changes in high-voltage insulation performance, and in some cases, even insulation failure. Real-time monitoring of the changes in high-voltage insulation performance and responding to variations in insulation resistance are crucial for ensuring the safe operation of electric vehicles.

Traditional insulation detection methods can be categorized into two types: online and offline [12]. The voltmeter readings are only accessible in an offline manner [13,14].

The disadvantages of this technique include a limited voltage range, complex operation, and unstable voltage output.

Online insulation detection includes the use of balanced bridge methods, unbalanced bridge methods, and signal injection methods [15,16]. The balanced bridge system is a constant measurement system, which is not suitable for scenarios where insulation resistance (IR) decreases simultaneously on both sides. The unbalanced bridge method can overcome the shortcomings of the balanced bridge method but significantly increases the cost of the measurement circuit [17,18]. The disadvantages of the bridge methods mainly include low robustness, low detection accuracy, poor sensitivity, complex circuitry, and high cost. Shen et al. [19] improved upon the traditional bridge method by employing a high-precision instrumentation amplifier and optimizing the algorithm. Although this approach enhanced the detection accuracy and reliability, it lacks versatility and is not suitable for high-voltage platforms.

The signal injection method is a technique that involves injecting a low-frequency signal into the battery pack and calculating insulation based on the feedback signal [12]. This method is easy to implement and can achieve real online detection, gradually becoming the mainstream testing method for insulation resistance in high-voltage systems of electric vehicles. However, this method requires simultaneous computation of the Kalman filter algorithm and the Recursive Least Squares (RLS) algorithm, which increases computational complexity and limits its application in electric vehicles. Song et al. proposed an equivalent circuit model for insulation resistance measurement in high-voltage direct current (HVDC) transmission systems based on low-voltage and low-frequency signal injection. They employed the Extended Kalman Filter (EKF) algorithm to estimate the insulation resistance of HVDC systems, which can accurately estimate the insulation resistance [20]. However, the EKF algorithm is prone to significant round-off errors in nonlinear processes [21]. Tian et al. [12] proposed a detection method based on the Kalman filter, considering that insulation detectors are susceptible to noise interference. They employed the Recursive Least-Squares (RLS) method to address the issue of varying detection results with battery pack voltage. Zhen [22] introduced a low-frequency signal injection method and designed a least-squares algorithm with a variable forgetting factor to rapidly and accurately estimate insulation resistance and Y-capacitance values. This method features fast response (average response time of 3 s), high robustness, high estimation accuracy (Root Mean Square Error, RMSE, less than 0.012), and strong interference resistance, making it suitable for the promotion in electric vehicles. Bukya et al. [23] proposed a VFF-RLS algorithm based on Field-Programmable Gate Array (FPGA) technology. The VFF-RLS-based FPGA technique effectively reduces errors when dealing with changes in battery terminal voltage and resistance conditions and can quickly monitor variations in Insulation Resistance (IR). It is evident that real-time online monitoring and alerting of the insulation status of the power battery system in electric commercial vehicles are essential for ensuring the overall vehicle safety. To achieve this, it is crucial to perform dynamic, real-time, and effective detection of the insulation resistance value of the power battery system. An alarm should be triggered when the insulation resistance value falls outside the safety range, and the controller should take timely safety measures to protect personal safety.

This article provides a battery insulation detection algorithm based on the bridge-balancing methodology, with further optimizations to develop an insulation monitoring system and enhanced algorithm tailored for commercial new energy vehicle (NEV) traction battery systems. The proposed system demonstrates robust applicability in high-voltage commercial vehicle environments, characterized by exceptional universality and measurement accuracy exceeding industry benchmarks.

2. Design of Insulation Inspection System for Commercial Vehicles

Due to the complex system and high-voltage platform of electric commercial vehicles, the signal injection method suffers from significant dynamic detection errors and long response times. An article detection system and dynamic insulation detection algorithm for the battery system of electric commercial vehicles are proposed. These are based on the bridge method, incorporating the principles of the latest national standards and the improvement methods suggested by Shen Yongpeng et al. [19]. The insulation detection circuit is integrated into the Battery Management System (BMS) [24–27].

3. Battery Insulation Detection Method Based on Bridge Method

The battery insulation detection method based on the bridge method is shown in Figure 1. The detection steps are as follows:

(1) Two voltmeters with the same internal resistance are simultaneously in parallel across the two terminals of the REESS and between the electrical platform; the higher voltage is read as U_1 , and the lower is read as U_1' , as shown in Figure 1b.

(2) After connecting a known unbalanced resistor R_0 to the end with a larger voltage, the voltages at this moment are then read as U_2 and U_2' , as shown in Figure 1c.

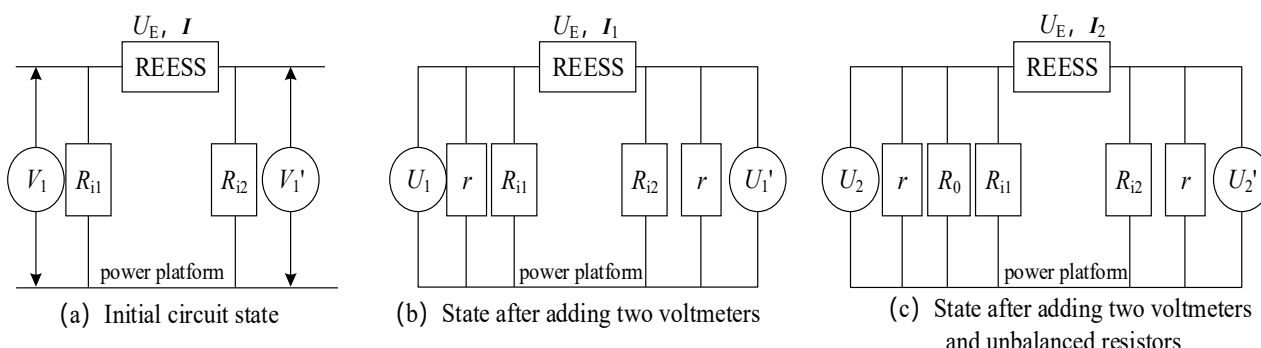


Figure 1. Battery Insulation Resistance Detection Principle Based on the Bridge Method. Notes: ① REESS (rechargeable electrical energy storage system) means a rechargeable energy storage system that can provide electrical energy; U_E means the electric potential of REESS, and I , I_1 , and I_2 mean the current flowing through the corresponding circuit. ② R_{i1} and R_{i2} denote the insulation resistance between the REESS and the electrical platform, and R_{i2} is the smaller of the resistance values, from which it is determined as the REESS insulation resistance R_i . ③ V_1 and V_1' indicate the voltages across R_{i1} and R_{i2} in an ideal state. ④ U_1 , U_1' , U_2 , and U_2' indicate the corresponding circuit voltmeter measurements. ⑤ r denotes the internal resistance of the corresponding voltmeter. ⑥ R_0 indicates unbalanced resistance.

According to Ohm's law and (b), the following can be obtained ("// is the parallel symbol):

$$\frac{U_1'}{U_1} = \frac{R_{i2}/r \bullet I_1}{R_{i1}/r \bullet I_1} \quad (1)$$

Metamorphosis must be:

$$R_{i1}/r = (R_{i2}/r) \frac{U_1'}{U_1} \quad (2)$$

According to Ohm's law and (c),

$$\frac{U_2'}{U_2} = \frac{R_{i2}/r \bullet I_2}{R_{i1}/r // R_0 \bullet I_2} \quad (3)$$

Substituting Equation (2) into Equation (3) yields:

$$\frac{R_{i2} \bullet r}{R_{i2} + r} = R_0 \left(\frac{U_2'}{U_2} - \frac{U_1'}{U_1} \right) \quad (4)$$

Rearranging the equation yields:

$$R_{i2} = \frac{\frac{1}{R_0 \left(\frac{U_2'}{U_2} - \frac{U_1'}{U_1} \right)} - \frac{1}{r}}{1} \quad (5)$$

The values of U_1 , U_1' , U_2 , and U_2' can be obtained through voltage measurement equipment. The values of R_0 and r are known. The value of R_{i2} can be calculated using Equation (5), which represents the insulation resistance value R_i of the entire vehicle.

But there are two problems with the method:

1. Detection accuracy is determined by the detection accuracy of U_1 , U_1' , U_2 , and U_2' . Due to the influence of the distribution capacitance, the higher the total battery voltage is, the longer the stability of U_2 and U_2' after incorporating the imbalanced resistor R_0 , and the greater the error that exists in the detection, which results in the greater the error in the calculated insulation resistance value.
2. When simultaneous insulation faults occur between the REESS ends and the electrical platform, only the smaller of the insulation resistances can be calculated, and it is not possible to calculate R_{i1} and R_{i2} at the same time.

Verification Standard for Insulation Monitoring Function of Electric Vehicles

R_x is defined as the target value for the insulation fault alarm, U_{REESS} is the current total voltage of the battery pack, and R_i is the current insulation resistance value of the whole vehicle. If the minimum insulation resistance value is required to be $100 \Omega/V$, R_x is defined in Equation (6) in the range for audible and visual alarms.

$$\frac{1}{\frac{1}{95U_{REESS}} - \frac{1}{R_i}} \leq R_x < \frac{1}{\frac{1}{100U_{REESS}} - \frac{1}{R_i}} \quad (6)$$

If the minimum required insulation resistance value is $500 \Omega/V$, then, if the value of R_x falls within the range specified by Equation (7), an audio-visual alarm will be triggered.

$$\frac{1}{\frac{1}{475U_{REESS}} - \frac{1}{R_i}} \leq R_x < \frac{1}{\frac{1}{500U_{REESS}} - \frac{1}{R_i}} \quad (7)$$

In this paper, the voltage platform of the commercial vehicle power battery system is 800 V, i.e., $U_{REESS} = 800$ V. Under normal circumstances, R_i is $10 M\Omega$ or more, allowing $1/R_i$ to be ignored; the actual design scheme will generally design a multi-level warning mechanism, as detailed in Table 1.

Table 1. Insulation warning mechanisms.

Fault Level	Resistance Range	Alarm Action
Class II	$76 k\Omega \leq R_x < 80 k\Omega$	audible and visual alarm
Class I	$380 k\Omega \leq R_x < 400 k\Omega$	insulation warning
/	$R_x \geq 400 k\Omega$	normal conditions, no alarm

4. Power Battery Insulation Detection Circuit Design and Estimation Algorithm for Commercial Vehicles

Aiming at the problems existing in the battery insulation detection method based on the bridge method, according to the special characteristics of commercial vehicles' working conditions, voltage platforms, and vehicle systems, we reviewed the existing mainstream insulation detection methods, and based on this method, we proposed an insulation resistance detection circuit for power batteries in commercial vehicles, as shown in Figure 2.

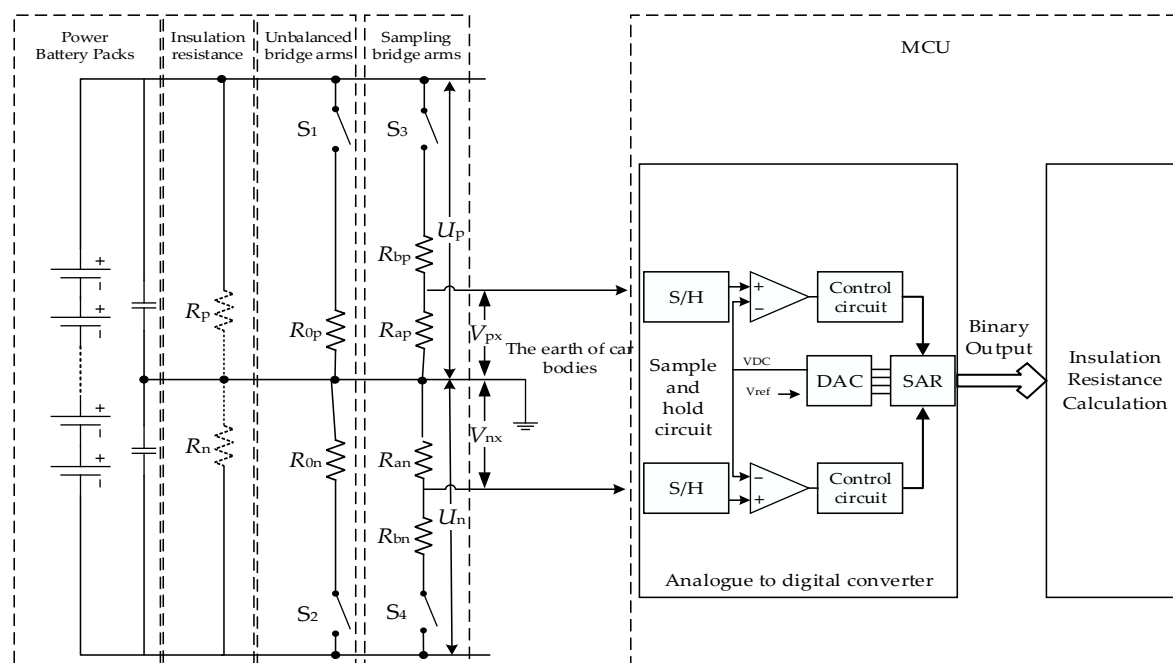


Figure 2. Dynamic Insulation Resistance Detection Circuit for Commercial Vehicle Power Battery. Notes: ① R_p indicates the insulation resistance between the positive bus of the power battery and the vehicle ground, and R_n indicates the insulation resistance between the negative bus of the power cell and the vehicle ground. ② S_1 , S_2 , S_3 , and S_4 are optical MOS to control the access and disconnection of the bridge arm. ③ R_0 is the unbalanced resistance, R_{0p} indicates the unbalanced resistance between the positive bus and vehicle ground, and R_{0n} indicates the unbalanced resistance between the negative bus and vehicle ground. ④ R_a is the voltage sampling resistor, R_b is the voltage divider resistor, R_{ap} and R_{bp} denote the voltage sampling resistor and voltage divider resistor between the positive busbar and the vehicle ground, and R_{an} and R_{bn} denote the voltage sampling resistor and voltage divider resistor between the negative busbar and the vehicle ground. ⑤ U_p indicates the voltage between the positive bus and vehicle ground, and U_n indicates the voltage between the negative bus and vehicle ground. ⑥ V_{px} indicates the voltage between R_{ap} and the vehicle ground, and V_{nx} indicates the voltage between R_{an} and the vehicle ground.

The circuit uses the vehicle ground as a reference and consists of five modules: power battery pack (including the Y capacitance of the whole vehicle), insulation resistance, unbalanced bridge arm, sampling bridge arm, and MCU. Among these, the unbalanced bridge arm, sampling bridge arm, and MCU modules constitute the hardware circuit components for the insulation resistance detection of the commercial vehicle's power battery. The unbalanced bridge arm, sampling bridge arm module consists of four optical MOS (MOSFET) switches, a pair made up of an imbalanced bridge arm and a resistance divider sampling arm, where $R_0 = R_{0p} = R_{0n}$, $R_a = R_{ap} = R_{an}$, and $R_b = R_{bp} = R_{bn}$. When all four switches are open, the insulation detection circuit can be disconnected from the positive and negative busbars, thereby preventing the insulation detection circuit from

affecting other circuits. The opening and closing of switches S_3 and S_4 are controlled through software settings, thereby controlling the termination and initiation of insulation detection. The opening and closing states of switches S_1 and S_2 are set to control the busbar end connected to the unbalanced resistor R_0 . The sampling bridge arm acquires V_p and V_n in different states by the resistor voltage divider. The MCU (Microcontroller Unit) acquires the AD value of the voltage signals, then performs signal processing, conversion, and calculates the insulation resistance value, and then makes corresponding alarm actions according to the fault mechanism. The method requires only three steps to calculate the insulation resistance value.

1. Positive unbalanced voltage acquisition

Close S_1 , S_3 , and S_4 ; disconnect S_2 to obtain U_{p1} , U_{n1} , V_{p1} , and V_{n1} ; the equivalent circuit is shown in Figure 3a, where $R_c = R_{ap} + R_{bp} = R_{an} + R_{bn}$, $R_p' = R_p // R_c$, $R_n' = R_n // R_c$, and according to Ohm's law, the following can be obtained:

$$\frac{U_{n1}}{U_{p1}} = \frac{\frac{V_{n1}(R_{an}+R_{bn})}{R_{an}} \bullet I_1}{\frac{V_{p1}(R_{ap}+R_{bp})}{R_{ap}} \bullet I_1} \quad (8)$$

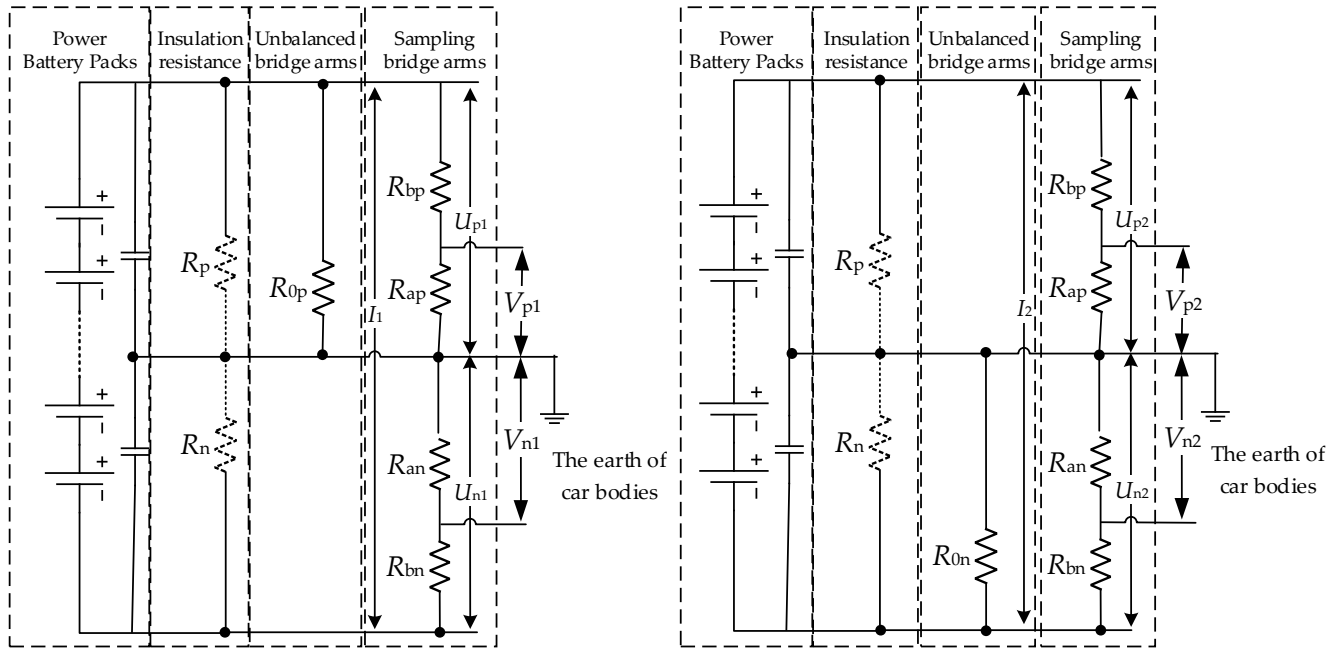
$$\frac{U_{n1}}{U_{p1}} = R_n' \bullet \left(\frac{1}{R_0} + \frac{1}{R_p'} \right) \quad (9)$$

2. According to Equations (9) and (10), the following can be obtained:

$$R_n' = \frac{V_{n1}}{V_{p1}} \bullet \left(\frac{R_0 \bullet R_p'}{R_0 + R_p'} \right) \quad (10)$$

3. Negative unbalanced voltage acquisition

Close S_2 , S_3 , and S_4 ; disconnect S_1 to obtain U_{p2} , U_{n2} , V_{p2} , and V_{n2} ; the equivalent circuit is shown in Figure 3b, and the following can be obtained:



(a) Equivalent circuit diagram with S_1 , S_3 and S_4 closed

(b) Equivalent circuit diagram with S_2 , S_3 and S_4 closed

Figure 3. Equivalent circuit diagram of power battery insulation detection circuit for commercial vehicles.

$$\frac{V_{p2}}{V_{n2}} = R_p' \left(\frac{1}{R_0} + \frac{1}{R_n'} \right) \quad (11)$$

Rearranging the equation yields:

$$R_p' = \frac{V_{p2}}{V_{n2}} \bullet \left(\frac{R_0 \bullet R_n'}{R_0 + R_n'} \right) \quad (12)$$

4. Estimation of insulation resistance

Substituting Equation (10) into Equation (11) yields:

$$R_p' = \frac{R_0 \bullet (V_{p2} \bullet V_{n1} - V_{p1} \bullet V_{n2})}{V_{n2} \bullet (V_{n1} + V_{p1})} \quad (13)$$

By replacing Formula Equation (12) and substituting Formula Equation (9), we obtain:

$$R_n' = \frac{R_0 \bullet (V_{p2} \bullet V_{n1} - V_{p1} \bullet V_{n2})}{V_{p1} \bullet (V_{n2} + V_{p2})} \quad (14)$$

Based on $R_c = R_{ap} + R_{bp} = R_{an} + R_{bn}$, $R_p' = R_p / R_c$, $R_n' = R_n / R_c$, we obtain:

$$R_p = \frac{1}{\frac{(V_{n1} + V_{p1}) \bullet V_{n2}}{R_0 \bullet (V_{p2} \bullet V_{n1} - V_{p1} \bullet V_{n2})} - \frac{1}{R_{ap} + R_{bp}}} \quad (15)$$

$$R_n = \frac{1}{\frac{(V_{n2} + V_{p2}) \bullet V_{p1}}{R_0 \bullet (V_{p2} \bullet V_{n1} - V_{p1} \bullet V_{n2})} - \frac{1}{R_{an} + R_{bn}}} \quad (16)$$

5. Software Workflow of Insulation Detection Algorithm

5.1. Software Flow of Battery Insulation Detection Algorithm Based on Bridge Method

The circuit corresponding to the battery insulation detection method based on the bridge method is shown in Figure 2, and the detailed software flowchart is shown in Figure 4; after the insulation detection starts, the process starts by closing switches S_3 and S_4 to calculate U_1 and U_1' . Next, close the switch corresponding to the larger value U_1 end (S_1 or S_2), then calculate U_2 and U_2' , and finally, calculate the insulation resistance value R_i according to Formula (5), where $r = R_{ap} + R_{bp} = R_{an} + R_{bn}$.

5.2. Dynamic Insulation Detection Algorithm Software Flow for Commercial Vehicles

The dynamic insulation detection algorithm for commercial vehicles designed in this paper can simultaneously collect the insulation resistance values between the two ends of REESS and the electric platform. It improves sampling accuracy under the dynamic working conditions (with Y capacitance) of the whole vehicle by cyclically collecting the AD values on R_{ap} and R_{an} , and calculating the corresponding U_p and U_n . The algorithm also assesses the three consecutive voltage deviation values of U_p and U_n . The workflow diagram of dynamic insulation detection is shown in Figure 5.

The detection process includes the following steps:

1. Initialization;
2. Close the positive unbalanced switch S_1 and the positive-negative sampling bridge arm S_3 and S_4 ;
3. Sample the AD values corresponding to V_{p1} and V_{n1} within 15 s and calculate V_{p1} , V_{n1} , U_{p1} , and U_{n1} ;
4. When the deviation of U_{p1} and U_{n1} is ≤ 1 V three times consecutively, take the last V_{p1} and V_{n1} corresponding to U_{p1} and U_{n1} as the final value;

5. If U_{p1} and U_{n1} do not satisfy the three consecutive deviations of ≤ 1 V in 15 s, then the maximal insulation value and the insulation fault will be reported;
6. Close the negative unbalanced switch S_2 and the positive-negative sampling bridge arm S_3 and S_4 ; cyclically sample the AD values corresponding to V_{p2} and V_{n2} within 15 s and calculate V_{p2} , V_{n2} , U_{p2} , and U_{n2} ; when the deviation of U_{p2} and U_{n2} is ≤ 1 V three times consecutively, take the last V_{p2} and V_{n2} corresponding to U_{p2} and U_{n2} as the final value; if U_{p2} and U_{n2} do not satisfy the three consecutive deviations of ≤ 1 V in 15 s, then the maximal insulation value and the insulation fault will be reported;
7. The final value of V_{p1} , V_{n1} , V_{p2} , V_{n2} , R_{ap} , R_{bp} , R_{an} , and R_{bn} is substituted into Equations (15) and (16) to calculate the insulation resistance of the positive and negative bus to the chassis. The detailed flow chart is shown in Figure 6.

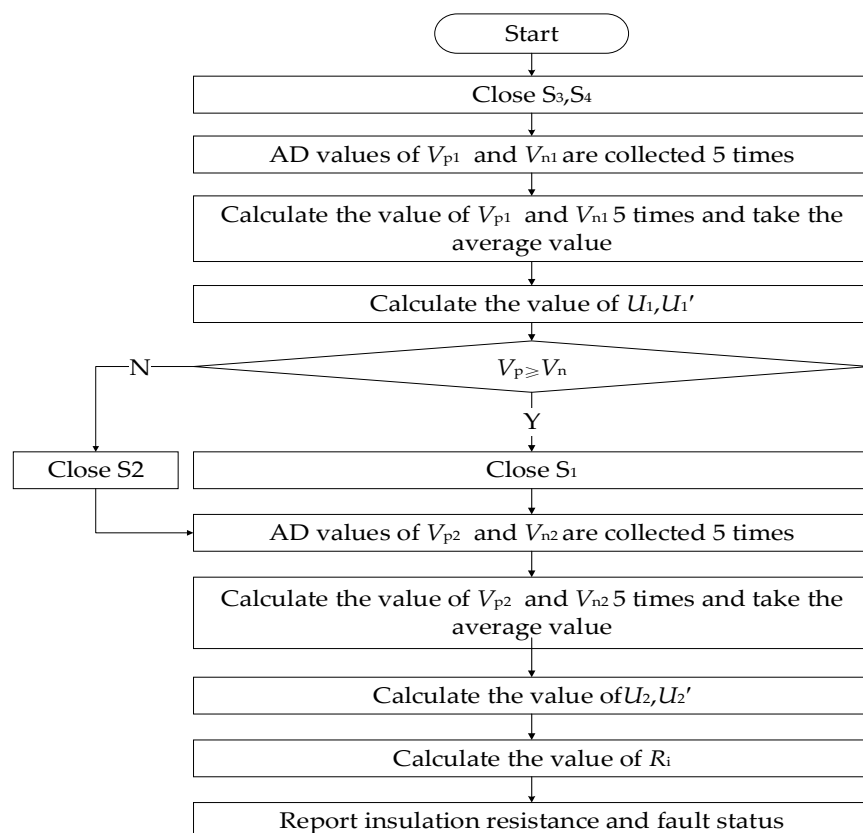


Figure 4. Flow chart of insulation testing and calculation.

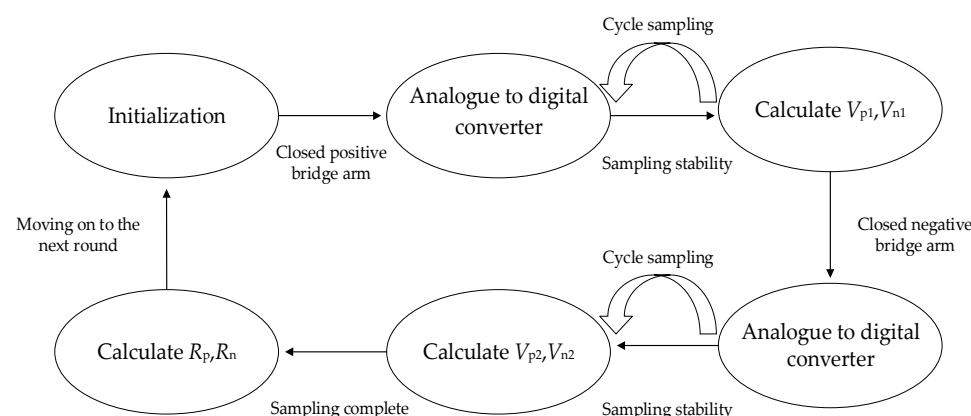


Figure 5. Schematic diagram of the workflow of self-dynamic insulation testing for commercial vehicles.

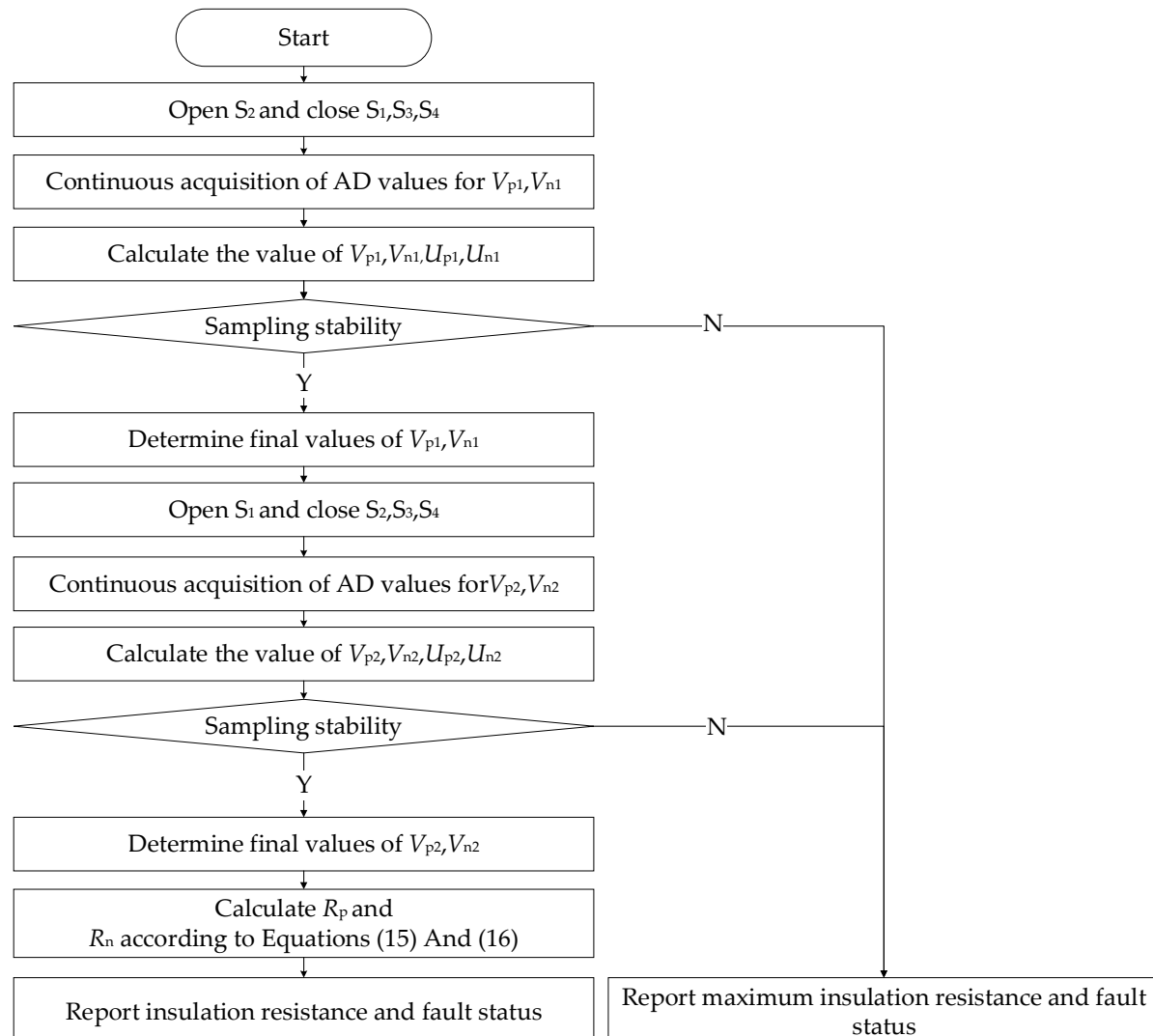


Figure 6. Detailed flowchart of adaptive dynamic insulation detection for commercial vehicles.

As can be seen in Figure 6, there are two differences between the adaptive dynamic insulation inspection process for commercial vehicles and the battery insulation inspection process based on the bridge method: ① Closing the positive end unbalanced arm and the negative end unbalanced arm, respectively, which is done in order to calculate the insulation resistances of the busbar on the chassis at both the positive and negative ends, instead of only calculating the insulation resistance of the busbar on the chassis at both the positive and negative ends of the chassis at the smaller one. ② A sampling stability determination mechanism was implemented, requiring the system to meet predefined stability criteria within 15 s before proceeding to subsequent processes. Failure to satisfy these conditions triggers an insulation sampling fault alarm, aiming to enhance measurement accuracy by ensuring signal integrity.

6. Validation of Dynamic Insulation Test Methods for Commercial Vehicles

To verify the accuracy of the dynamic insulation detection method for new energy commercial vehicles and compare it with the battery insulation detection method based on the bridge method, a test bench (as shown in Figure 7) was established for validation. Under the same experimental conditions and hardware circuitry, tests were conducted using both the battery insulation detection method based on the bridge method and the dynamic

insulation detection method for new energy commercial vehicles. The experiment uses a high-voltage power supply to simulate the battery pack voltage, which was set to 800 V. The developed circuit was integrated into the main controller of the battery management, and the programmable power supply was used to supply power to the main control board system; the power supply voltage was set to 24 V. In the experiment, the adjustable resistor box was used to connect resistors with different resistance values in parallel between the battery terminals and the vehicle ground (the vehicle body), thereby simulating different insulation resistance scenarios. Meanwhile, research revealed that the actual Y capacitance of the electric commercial vehicle has two kinds: 470 nf and 690 nf (formed by the parallel 470 nf and 220 nf). The experiment simulates the vehicle's Y capacitance by incorporating 470 nf and 690 nf safety capacitors into the test circuit in parallel, respectively.

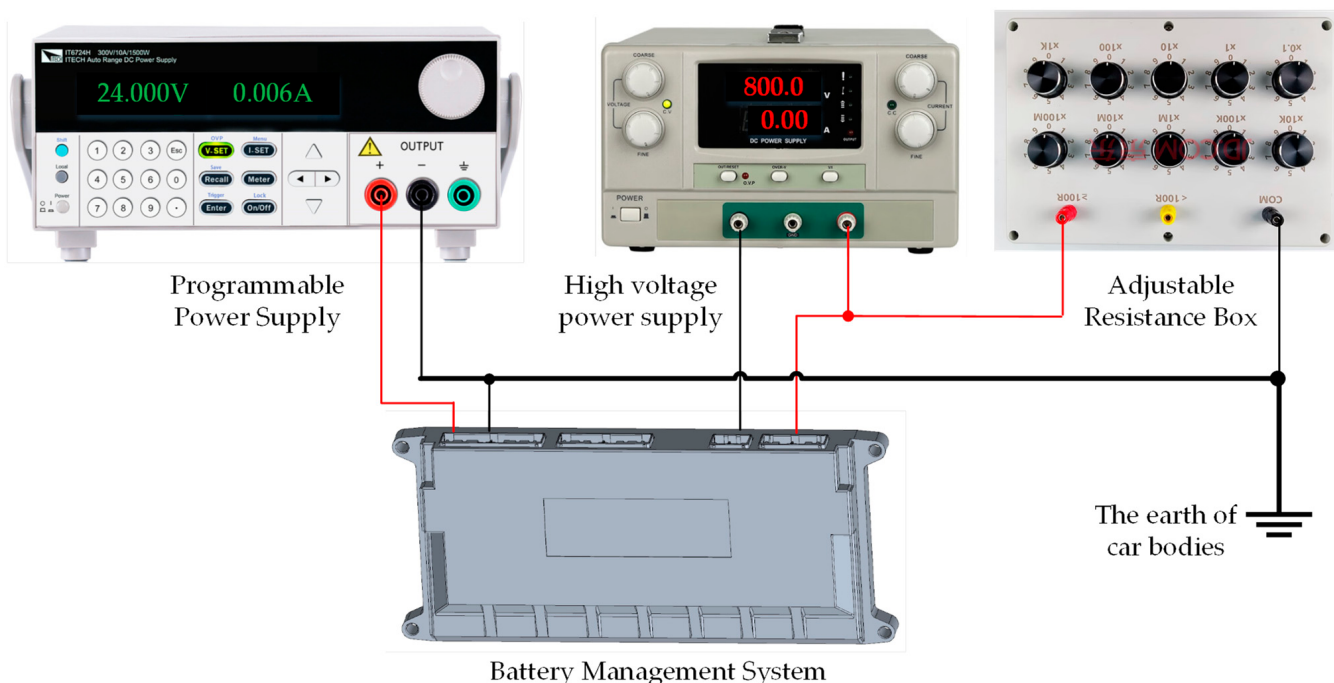


Figure 7. Insulation test stand.

The test is carried out in four stages, corresponding to four different test states. State 1 is to access the simulated adjustable insulation resistance between the vehicle ground and the positive battery terminal or the vehicle ground and the negative battery terminal; state 2 is to access the simulated insulation resistance between the vehicle ground and the positive battery terminal, the vehicle ground and the negative battery terminal at one end, and a fixed insulation resistance at the other end; state 3 is to access 470 nf Y capacitance between state 3 is based on state 1, and at the same time, between the vehicle ground and the battery positive end, the vehicle ground and the battery negative end each has access to the 470 nf Y capacitor; state 4 is based on state 1, and at the same time, between the vehicle ground and the battery positive end, the vehicle ground and the battery negative end each has access to the 690 nf Y capacitor; the specific operation steps are shown below:

State 1: At first, variable resistor R was connected between the positive terminal of the battery and the vehicle ground; the negative terminal of the battery was left disconnected; measurements were run. Then, variable resistor R was connected between the negative terminal of the battery and the vehicle ground; the positive terminal of the battery was left disconnected; again, measurements were run. The insulation resistance value and the error data of the test are shown in Table 2.

Table 2. State 1 test data.

Detection Methods	R Setting Value (kΩ)	R _p Measured Value (kΩ)	R _p Error	R _n Measured Value (kΩ)	R _n Error
Dynamic Insulation Test Method with unbalanced bridge	50	49	−2.00%	46	−8.00%
	100	99	−1.00%	91	−9.00%
	300	294	−2.00%	287	−4.33%
	500	484	−3.20%	472	−5.60%
	760	727	−4.34%	714	−6.05%
Dynamic Insulation Test Method for Electric Commercial Vehicles	50	50	0.00%	50	0.00%
	100	100	0.00%	100	0.00%
	300	301	0.33%	297	−1.00%
	500	500	0.00%	491	−1.80%
	760	761	0.13%	749	−1.45%

State 2: Firstly, variable resistor R was connected between the positive terminal of the battery and the vehicle ground, and a fixed resistor between the negative end of the battery and the vehicle ground, with a resistance value of 1.352 MΩ. Then, variable resistor R was connected between the negative terminal of the battery and the vehicle ground, and a fixed resistor between the positive end of the battery and the vehicle ground, with a resistance value of 1.352 MΩ. The insulating resistance values and the error data of the test are shown in Table 3.

Table 3. State 2 test data.

Sensing Methodologies	R _p and R _n Setting Value (kΩ)	R _p Measured Value (kΩ)	R _n Measured Value (kΩ)	R _p Error	R _n Error
Dynamic Insulation Test Method with unbalanced bridge	50, 1352	49	/	−2.00%	/
	100, 1352	100	/	0.00%	/
	300, 1352	293	/	−2.33%	/
	500, 1352	478	/	−4.40%	/
	760, 1352	717	/	−5.66%	/
	1352, 50	/	50	/	0.00%
	1352, 100	/	97	/	−3.00%
	1352, 300	/	287	/	−4.33%
	1352, 500	/	473	/	−5.40%
	1352, 760	/	713	/	−6.18%
Dynamic Insulation Test Method for Electric Commercial Vehicles	50, 1352	49	1353	−2.00%	0.07%
	100, 1352	100	1357	0.00%	0.37%
	300, 1352	300	1353	0.00%	0.07%
	500, 1352	494	1345	−1.20%	−0.52%
	760, 1352	755	1335	−0.66%	−1.26%
	1352, 50	1351	48	−0.07%	−4.00%
	1352, 100	1322	98	−2.22%	−2.00%
	1352, 300	1343	295	−0.67%	−1.67%
	1352, 500	1344	488	−0.59%	−2.40%
	1352, 760	1347	746	−0.37%	−1.84%

Note: The bridge-based battery insulation detection methodology exhibits a critical limitation: it exclusively quantifies the insulation resistance at the terminal with lower resistivity, while failing to accurately measure the counterpart at the higher-resistance terminal due to inherent systemic constraints, according to the columns with “/”.

State 3: A 470 nF safety capacitor was connected in parallel between the positive end of the battery and the vehicle ground, as well as between the negative end of the battery and the vehicle ground, to simulate the Y capacitance of the whole vehicle. A variable resistor was sequentially connected between the positive end of the battery and the vehicle ground, the negative end of the battery and the vehicle ground, with the other end suspended in the air. The tested insulation resistance value and error data are shown in Table 4.

Table 4. State 3 test data.

Detection Methods	R Setting Value (kΩ)	R _p Measured Value (kΩ)	R _p Error	R _n Measured Value (kΩ)	R _n Error
Dynamic Insulation Test Method with unbalanced bridge	50	48	-4.00%	42	-16.00%
	100	99	-1.00%	91	-9.00%
	300	284	-5.33%	245	-18.33%
	500	440	-12.00%	350	-30.00%
	760	597	-21.45%	495	-34.87%
Dynamic Insulation Test Method for Electric Commercial Vehicles	50	50	0.00%	49	-2.00%
	100	99	-1.00%	98	-2.00%
	300	297	-1.00%	294	-2.00%
	500	493	-1.40%	481	-3.80%
	760	743	-2.24%	733	-3.55%

State 4: To simulate the vehicle Y capacitor, a 690 nF safety capacitor was connected in parallel between the positive terminal of the battery and the vehicle ground, and between the negative terminal of the battery and the vehicle ground. A variable resistor was sequentially connected between the positive terminal of the battery and the vehicle ground, and between the negative terminal of the battery and the vehicle ground, while no resistor was connected at the other end. The measured insulation resistance values and error data are shown in Table 5.

Table 5. State 4 test data.

Detection Methods	R setting Value (kΩ)	R _p Measured Value (kΩ)	R _p Error	R _n Measured Value (kΩ)	R _n Error
Dynamic Insulation Test Method with unbalanced bridge	50	49	-2.00%	41	-18.00%
	100	98	-2.00%	79	-21.00%
	300	262	-12.67%	191	-36.33%
	500	366	-26.80%	266	-46.80%
	760	454	-40.26%	310	-59.21%
Dynamic Insulation Test Method for Electric Commercial Vehicles	50	49	-2.00%	49	-2.00%
	100	95	-5.00%	97	-3.00%
	300	296	-1.33%	293	-2.33%
	500	484	-3.20%	476	-4.80%
	760	732	-3.68%	723	-4.87%

The results from the four sets of data demonstrate that, under identical hardware circuit and test environment conditions, the dynamic insulation detection method for new

energy commercial vehicles is capable of not only calculating the insulation resistance between the positive or negative terminal of the battery and the vehicle ground, but also, in the event of simultaneous insulation abnormalities between the positive terminal of the battery, the negative terminal of the battery, and the vehicle ground, it can accurately calculate the insulation resistance among these components. Furthermore, an additional advantage of this dynamic insulation detection method is its optimization of the sampling method and algorithm in accordance with the characteristics of the commercial vehicle's high-voltage platform and large Y capacitance, thereby enhancing the estimation accuracy. Verification has confirmed that the detection error of this method remains within 5% across various operating conditions. The application of this detection method significantly improves the insulation detection accuracy of commercial vehicles under the four defined operational scenarios, reduces the likelihood of false alarms for insulation faults, and thereby better ensures the personal safety of passengers.

In summary, the dynamic insulation testing method for electric commercial vehicles has better testing accuracy than the battery insulation detection method based on the bridge method, and compared with other existing insulation testing methods for electric passenger vehicles, this testing method can better meet the insulation testing needs of commercial vehicles.

7. Conclusions

The paper introduces two insulation detection methods and proposes a new dynamic insulation detection method applicable to commercial electric vehicles with high-voltage platforms, which can dynamically calculate the equivalent insulation resistance value of the positive and negative terminals of the high-voltage battery to the ground of the vehicle body in real time. The testing proves that the detection accuracy is within 5% under various working conditions, and at the same time, based on different insulation threshold values, insulation fault early warning can be achieved, which enables both single-end insulation fault alarms and dual-end insulation fault alarms. This method has been effectively implemented in the 800 V power battery system.

At the same time, the battery management system controller applying this testing method has already completed batch mounting on the new energy commercial vehicles of famous brands in China, which can carry out real-time and accurate testing of the insulation resistance value of the whole vehicle under various working conditions and provide fault alarms when there is an insulation risk in the vehicle to ensure the personal safety of the vehicle occupants. For traction battery systems operating within 800–1000 V platforms, the dynamic insulation monitoring methodology achieves accurate detection and early warning when insulation resistance resides in the range of 0–600 k Ω (equivalent to 600 Ω/V under the rated voltage).

Author Contributions: Methodology, D.S. and X.Z.; Software, X.Z.; Investigation, Y.H.; Data curation, F.G. and Y.H.; Writing—original draft, D.S.; Writing—review & editing, F.G. and X.Z. All authors have read and agreed to the published version of the manuscript.

Funding: This work has been supported by the Zhejiang Provincial Emergency Department Project (Grant No. 2024YJ023) and the Key R&D Program of the Ministry of Science and Technology (Grant No. 2023YFB3209805), China.

Data Availability Statement: The original contributions presented in this study are included in the article. Further inquiries can be directed to the corresponding author.

Acknowledgments: The authors are also thankful for the help of the Hunan New Energy Heavy Truck Power Systems Engineering Technology Research Center.

Conflicts of Interest: Authors Feng Guo and Danping She were employed by the company Hunan Xingbida Wanglian Technology Co., Ltd. The remaining authors declare that the research was conducted in the absence of any commercial or financial relationships that could be construed as a potential conflict of interest.

References

- Wang, X.; Hao, H.; Liu, J.; Huang, T.; Yu, A. A novel method for preparation of macroporous lithium nickel manganese oxygen as cathode material for lithium ion batteries. *Electrochim. Acta* **2011**, *56*, 4065–4069.
- Xie, Z.; Ellis, S.; Xu, W.; Dye, D.; Zhao, J.; Wang, Y. A novel preparation of core–shell electrode materials via evaporation-induced self assembly of nanoparticles for advanced Li-ion batteries. *Chem. Commun.* **2015**, *51*, 15000–15003. [[CrossRef](#)] [[PubMed](#)]
- Zeng, Y.K.; Zhao, T.S.; Zhou, X.L.; Zeng, L.; Wei, L. The effects of design parameters on the charge-discharge performance of iron-chromium redox flow batteries. *Appl. Energy* **2016**, *182*, 204–209. [[CrossRef](#)]
- Jiang, J.; Ji, H. Study of insulation monitoring device for DC system based on multi-switch combination. In Proceedings of the 2nd International Symposium on Computational Intelligence and Design, Changsha, China, 12–14 December 2009; pp. 429–433.
- Li, C.; Luo, S.; Cole, C.; Spiriyagin, M. An overview: Modern techniques for railway vehicle on-board health monitoring systems. *Veh. Syst. Dyn.* **2017**, *55*, 1045–1070. [[CrossRef](#)]
- Chiang, Y.-H.; Sean, W.-Y.; Huang, C.-Y.; Chiang Hsieh, L.-H. Adaptive control for estimating insulation resistance of high-voltage battery system in electric vehicles. *Environ. Prog. Sustain. Energy* **2017**, *36*, 1882–1887. [[CrossRef](#)]
- Li, H.; Li, Z.; Lin, F.; Chen, Y.; Liu, D.; Wang, B. Measurement and analysis of insulation resistance of metallized polypropylene film capacitor under high electric field. In Proceedings of the IEEE International Power Modulator and High Voltage Conference (IPMHVC), San Diego, CA, USA, 3–7 June 2012; pp. 617–619.
- Torkaman, H.; Karimi, F. Measurement variations of insulation resistance/polarization index during utilizing time in HV electrical machines—A survey. *Measurement* **2015**, *59*, 21–29. [[CrossRef](#)]
- David, E.; Soltani, R.; Lamarre, L. PDC measurements to assess machine insulation. *IEEE Trans. Dielectr. Electr. Insul.* **2010**, *17*, 1461–1469. [[CrossRef](#)]
- Rui, R.; Cotton, I. Impact of low pressure aerospace environment on machine winding insulation. In Proceedings of the IEEE International Symposium on Electrical Insulation, San Diego, CA, USA, 6–9 June 2010; pp. 1–5.
- Du, B.X.; Yamano, Y. Effects of atmospheric pressure on DC resistance to tracking of polymer insulating materials. *IEEE Trans. Dielectr. Electr. Insul.* **2005**, *12*, 1162–1171. [[CrossRef](#)]
- Tian, J.; Wang, Y.; Yang, D.; Zhang, X.; Chen, Z. A real-time insulation detection method for battery packs used in electric vehicles. *J. Power Sources* **2018**, *385*, 1–9. [[CrossRef](#)]
- Dai, Q.; Zhu, Z.; Huang, D.; Du, M.; Wei, K. Insulation Detection of Electric Vehicle Batteries. *AIP Conf. Proc.* **2018**, *1971*, 040021.
- Wang, Y.; Tian, J.; Chen, Z.; Liu, X. Model based insulation fault diagnosis for lithium-ion battery pack in electric vehicles. *Measurement* **2019**, *131*, 443–451.
- Chiang, Y.-H.; Sean, W.-Y. Adaptive Control for Estimating Insulation Resistance of High-Voltage Battery System in Electric Vehicles. In *New Trends in Electrical Vehicle Powertrains*; IntechOpen: London, UK, 2019.
- Pei, X.; Hu, X.; Liu, W.; Chen, Z.; Yang, B. State Estimation of Vehicle’s Dynamic Stability Based on the Nonlinear Kalman Filter. *Automot. Innov.* **2018**, *1*, 281–289.
- Wen, F.; Pei, W.; Li, Q.; Chu, Z.; Zhao, W.; Wu, S.; Zhang, X.; Han, C. Insulation Monitoring of Dynamic Wireless Charging Network Based on BP Neural Network. *World Electr. Veh. J.* **2021**, *12*, 129. [[CrossRef](#)]
- Pande, A.S.; Soni, B.P.; Bhadane, K.V. Electrical Models for EV’s Batteries: An Overview and Mathematical Design of RC Network. *Inst. Eng. India Ser. B* **2023**, *104*, 533–547.
- Shen, Y.P.; Liu, A.K.; Cui, G.Z. Design of an online insulation resistance detection system for electric vehicles using an unbalanced bridge. *J. Light Ind.* **2018**, *33*, 10.
- Zhang, X.; Wang, Y.; Liu, C.; Chen, Z. A novel approach of remaining discharge energy prediction for large format lithium-ion battery pack. *J. Power Sources* **2017**, *343*, 216–225.
- Song, C.; Shao, Y.; Song, S.; Peng, S.; Zhou, F.; Chang, C.; Wang, D. Insulation resistance monitoring algorithm for battery pack in electric vehicle based on extended Kalman filtering. *Energies* **2017**, *10*, 714. [[CrossRef](#)]
- Chen, Z.; Cui, W.; Cui, X.; Qiao, H.; Lu, H.; Qiu, N. A new method of insulation detection on electric vehicles based on a variable forgetting factor recursive least squares algorithm. *IEEE Access* **2021**, *9*, 73590–73607.
- Bukya, M.; Padma, B.; Kumar, R.; Mathur, A.; Prasad, N. FPGA-Based VFF-RLS Algorithm for Battery Insulation Detection in Electric Vehicles. *World Electr. Veh. J.* **2024**, *15*, 129. [[CrossRef](#)]
- Yang, S. An insulation resistance detection method in battery management system. *Automot. Util. Technol.* **2023**, *48*, 6–11.
- Lv, Z. Design of insulation detection method for electric vehicles based on unbalanced bridge method. *Electron. Technol. Softw. Eng.* **2019**, *3*, 245–249.

26. Qin, Z.; Zhao, L.; Wang, X.; Yang, G. Discussion on the improvement of insulation resistance performance requirements and test methods for the whole vehicle in the new version of GB 18384. *Automot. Electr. Appl.* **2022**, *9*, 75–76, 80.
27. Gao, G.; Li, L.; Yu, Q.; Li, R. Research on the formula for calculating insulation resistance and alternative methods for GB 18384-2020. *China Stand.* **2023**, *4*, 49–51, 56.

Disclaimer/Publisher’s Note: The statements, opinions and data contained in all publications are solely those of the individual author(s) and contributor(s) and not of MDPI and/or the editor(s). MDPI and/or the editor(s) disclaim responsibility for any injury to people or property resulting from any ideas, methods, instructions or products referred to in the content.